Monthly Notices
of the
ROYAL ASTRONOMICAL SOCIETY

MNRAS **448,** 1807–1815 (2015) doi:10.1093/mnras/stv109

The effects of methanol on the trapping of volatile ice components

Daren J. Burke* and Wendy A. Brown

Division of Chemistry, University of Sussex, Falmer, Brighton, BN1 9QJ, UK

Accepted 2015 January 13. Received 2014 December 23; in original form 2014 December 23

ABSTRACT

The evaporation of icy mantles, which have been formed on the surface of dust grains, is acknowledged to give rise to the rich chemistry that has been observed in the vicinity of hot cores and corinos. It has long been established that water ice is the dominant species within many astrophysical ices. However, other molecules found within astrophysical ices, particularly methanol, can influence the desorption of volatile species from the ice. Here we present a detailed investigation of the adsorption and desorption of methanol-containing ices, showing the effect that methanol has on the trapping and release of volatiles from model interstellar ices. OCS and CO_2 have been used as probe molecules since they have been suggested to reside in water-rich and methanol-rich environments. Experiments show that methanol fundamentally changes the desorption characteristics of both OCS and CO_2, leading to the observation of mainly codesorption of both species with bulk water ice for the tertiary ices and causing a lowering of the temperature of the volcano component of the desorption. In contrast, binary ices are dominated by standard volcano desorption. This observation clearly shows that codepositing astrophysically relevant impurities with water ice, such as methanol, can alter the desorption dynamics of volatiles that become trapped in the pores of the amorphous water ice during the sublimation process. Incorporating experimental data into a simple model to simulate these processes on astrophysical timescales shows that the additional methanol component releases larger amounts of OCS from the ice mantle at lower temperatures and earlier times. These results are of interest to astronomers as they can be used to model the star formation process, hence giving information about the evolution of our Universe.

Key words: astrochemistry – molecular processes – methods: laboratory – ISM: molecules.

1 INTRODUCTION

Sulphur-bearing species have been proposed as good evolutionary tracers of star-forming regions (Codella et al. 2006). However, uncertainties exist regarding the form that sulphur takes in the interstellar medium (ISM). In particular, due to the abundance of atomic hydrogen, it is often assumed that H_2S should be the most abundant sulphur-containing species in the ISM. However, H_2S has not been detected in the solid phase (Boogert et al. 2000) and instead carbonyl sulphide (OCS) is suggested to be the main reservoir of sulphur on dust grains (Codella et al. 2006). OCS has been detected in the condensed phase towards protostar W33A (Gibb et al. 2000), within our own Solar system in planetary atmospheres such as Jupiter (Lellouch et al. 1995) and Venus (Mills et al. 2007; Yung et al. 2009) and within cometary comae (Ehrenfreund et al. 1997; DelloRusso et al. 1998; Bockelee-Morvan et al. 2000). Identification of OCS in interstellar ices occurs via the C–O vibrational band at 4.9 μm, which has been shown in the laboratory to be best reproduced by OCS in the presence of methanol-containing ice (Palumbo et al. 1995, 1997).

Gas-phase methanol is ubiquitous in astrophysical environments and is found in many regions including cold clouds, hot cores and corinos, Galactic Centre, dense clouds and stellar outflows (Herbst & van Dishoeck 2009). Solid methanol is also widespread and is found in interstellar ices (Gibb et al. 2000), cometary nuclei (Bockelee-Morvan et al. 2000) and trans-Neptunian objects (Cruikshank et al. 1998; Merlin et al. 2012). Compared to other molecules, the abundance of methanol ice varies widely depending on the environment, ranging from as low as 5 per cent with respect to water in dark clouds to approximately 20–30 per cent near high- and low-mass protostars (Grim et al. 1991; Dartois et al. 1999; Pontoppidan et al. 2003).

As well as OCS and methanol, astrophysical ices also contain water, usually as the major component (Whittet 1993), along with other less abundant species. At the temperatures at which most astrophysical ices are found, water exists as amorphous solid water (ASW; Klinger 1983), but has also been detected in crystalline

* **E-mail**: darenburke@hotmail.com

forms (Jewitt & Luu 2004; Merlin et al. 2007). Laboratory studies have shown that water plays a major role in the desorption of various species within the ice, causing the trapping and retention of volatile ice components (Collings et al. 2004). It is becoming increasingly clear that the usual practice of investigating binary (two-component) ice mixtures does not always give an accurate description of the desorption characteristics of the ice, and it is also necessary to investigate the behaviour of multicomponent ices (Bar-Nun et al. 1988; Notesco & Bar-Nun 2000; Martín-Doménech et al. 2014). As a first step towards this goal, we have undertaken a detailed laboratory study of the thermal desorption of tertiary ices containing water and methanol, using OCS as a probe molecule. Our study shows that incorporating methanol as a core component of laboratory model ices significantly alters the trapping and release of volatiles, such as OCS, from water-rich ices.

We have previously investigated the desorption of OCS from astrophysically relevant binary ice systems containing OCS and water ice (Burke & Brown 2010) and have shown that OCS traps within pure water ice. Laboratory studies have also investigated methanol:water ices (Blake et al. 1991; Notesco & Bar-Nun 2000; Souda 2007; Wolff et al. 2007) and in some cases have shown that methanol alters the crystallization kinetics of ASW during the thermally induced phase transition to crystalline ice (CI). Since this phase transition plays an important role in the release of volatile species within water-rich interstellar ices during the warm-up phase, it is important to understand the role that methanol plays in dictating the thermal desorption of astrophysical ice species.

This study uses temperature programmed desorption (TPD) and reflection absorption infrared spectroscopy (RAIRS) to study the influence of methanol on the desorption of OCS from a carbonaceous model dust grain surface. Initial laboratory experiments establish the behaviour of binary ices consisting of OCS:water and OCS:methanol. We then go on to study tertiary ices containing OCS, water and methanol. The experimental data show that methanol clearly influences the desorption of OCS, and we compare these results with data for CO_2 desorption from water and methanol-containing ices also adsorbed on a carbonaceous surface (Edridge et al. 2013). The experimental data are then incorporated into a simple model to simulate the modified desorption of OCS from the tertiary ices, when compared to binary ices, at astrophysical temperatures and time-scales.

2 EXPERIMENTAL METHODS

Experiments were performed in an ultrahigh vacuum (UHV) chamber with a base pressure of $\leq 2 \times 10^{-10}$ mbar. Model interstellar ices were grown *in situ* on a highly oriented pyrolytic graphite (HOPG) surface, with a base temperature between 20 and 30 K. The HOPG sample was cleaned before each experiment by annealing to 300 K in UHV for 3 min. Sample cleanliness was confirmed by the absence of any desorption during TPD experiments performed with no dosage. Ices were grown on the HOPG via background deposition by a pair of high-precision leak valves. Gas doses are given in Langmuir (L_m), where 1 $L_m = 1 \times 10^{-6}$ mbar s. Two-component (binary) ices were grown either by sequential deposition from two separate leak valves (for layered ices) or by simultaneous deposition from two leak valves (for mixed, codeposited, ices). For layers of OCS adsorbed on CI or crystalline methanol, the underlying ices were grown by deposition of the relevant species onto the HOPG sample held at base temperature followed by annealing to 130 or 125 K for 6 min for the water and methanol, respectively. The sample was then cooled, before depositing OCS onto the CI at base temperature. Crystalline water or methanol ices were confirmed by RAIRS. Three-component (tertiary) mixed and layered ices were grown by simultaneous deposition of OCS from one leak valve and a pre-mixed water:methanol mixture from the second leak valve. The composition in the vapour phase was measured by recording a mass spectrum during the exposure. The actual percentage of methanol, water and OCS in the ice mixtures was determined by integrating the area under the resulting dose curves and correcting for mass spectrometer sensitivities to each species. Ice thicknesses are estimated to range from monolayers at the lowest exposures to around 20 Å for the thickest ices (100 L_m). Ices were studied using a combination of TPD and RAIRS. RAIR spectra were taken at a resolution of 4 cm^{-1} and are the result of the coaddition of 256 scans. For the annealed RAIRS experiments, the sample temperature was raised and held for 3 min before cooling back to the base temperature where a spectrum was recorded. TPD spectra were recorded at a heating rate of 0.50 K s^{-1}.

3 RESULTS

Fig. 1 shows the thermal desorption of OCS from three different binary water ice configurations; from the surface of CI (panel D), from the surface of ASW (panel C) and finally from a codeposited mixed OCS:water ice (panel B). In each case, the ratio between water and OCS was ∼10:1 as determined by mass spectrometry during ice deposition. Clearly, the OCS desorption depends on the ice configuration. On CI, desorption is characterized by a single sharp peak at 85 K. However, when OCS is adsorbed on ASW two main peaks are observed. The lower temperature peak is broad and centred around 95 K, and a sharper more intense feature is seen at 158 K. There is also a very small feature at 171 K. For the codeposited ices, OCS desorption is dominated by a main peak at 158 K, with a high-temperature feature at 171 K. In addition, as shown in the inset, desorption of OCS from a mixed ice occurs in a broad temperature range starting from 90 K and extending to the main desorption feature.

Comparison of all three ice configurations with the ASW TPD (Fig. 1A) allows assignment of the OCS desorption features. The low-temperature peak observed for binary layered ices is assigned to desorption from the surface of the water ice. For CI, OCS desorption is almost identical to that observed from clean HOPG (Burke & Brown 2010). Clearly, the porous nature of the ASW alters the desorption of this feature, causing it to broaden and increase in temperature due to the heterogeneity of the surface, when compared to desorption from HOPG.

The peak observed at 158 K in both the layered ASW and codeposited OCS ices is coincident with the low-temperature shoulder on the leading edge of the water TPD, which is characteristic of the phase transition of ASW to CI (Smith et al. 1997). Hence, the dominant feature in the two binary ice configurations is assigned to the release of OCS from the water lattice as the phase transition occurs, so-called volcano desorption (Smith et al. 1997). This volcano desorption has been observed for a range of other astrophysically relevant molecules (Ayotte et al. 2001; Collings et al. 2004; Burke & Brown 2010). For the layered amorphous water ice, this feature occurs as a result of OCS becoming trapped within the pores of ASW as the water undergoes a structural rearrangement prior to the phase transition. The high-temperature peak observed at 171 K, which is more dominant in the mixed ice, is coincident with the desorption of CI and is therefore assigned to the codesorption of OCS that becomes trapped within the water matrix following the phase transition. The complex desorption that occurs from 90 to

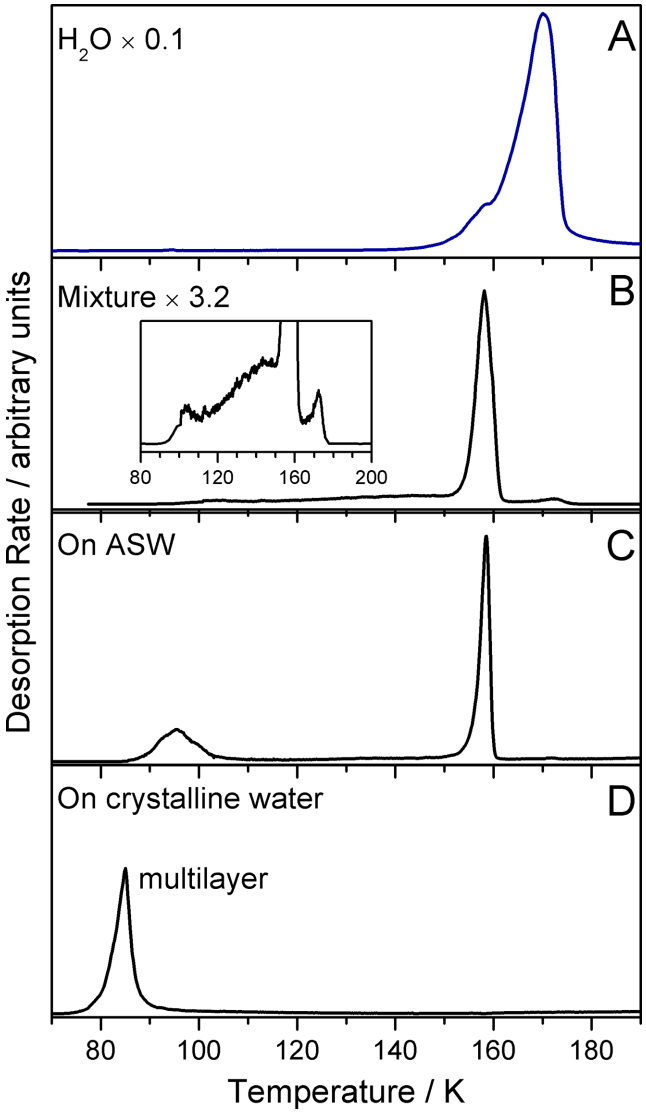

Figure 1. TPD spectra for various configurations of OCS and water-containing ices adsorbed on HOPG. (A) shows the desorption of water from the layered OCS/ASW ice. (B) shows the desorption of 100 L_m of a mixed OCS:water ice (10 per cent OCS) adsorbed on HOPG. The inset shows a close up of the 80–200 K temperature range, showing the desorption of OCS prior to the volcano desorption. (C) shows the desorption of 10 L_m of OCS adsorbed on top of 100 L_m of ASW grown on HOPG. (D) shows 10 L_m of pure OCS adsorbed directly onto the surface of CI.

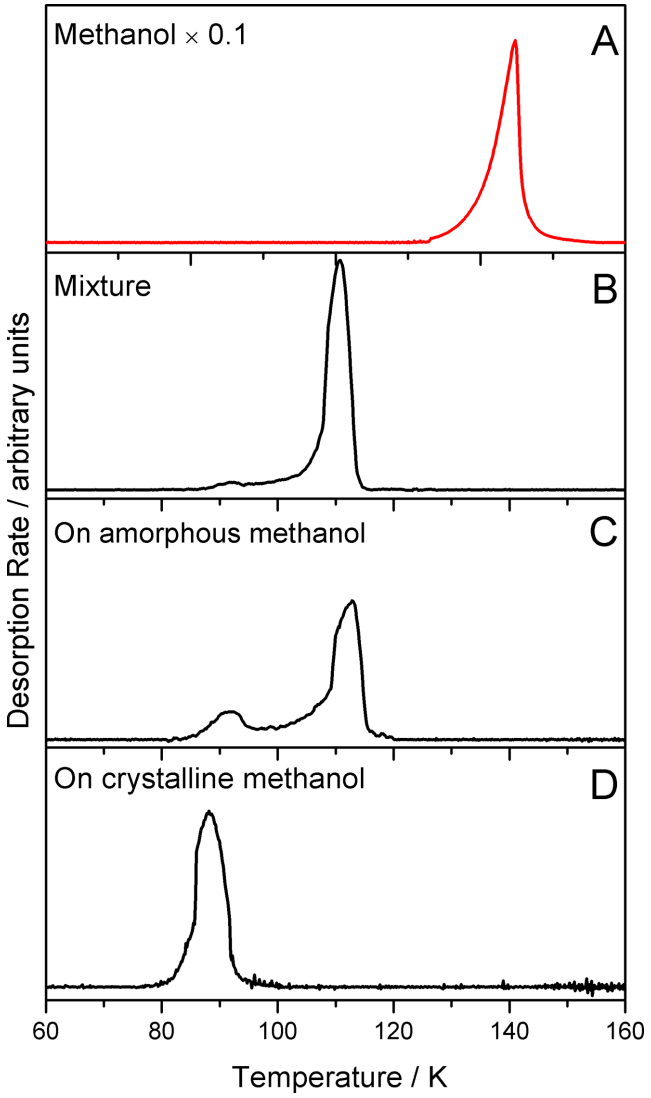

Figure 2. TPD spectra for various configurations of OCS and methanol binary ices adsorbed on HOPG. (A) shows the desorption of methanol from a mixed OCS:methanol ice. (B) shows the desorption of OCS from a 100 L_m mixed OCS:methanol (10 per cent OCS) ice. (C) shows the desorption of 10 L_m of OCS from an amorphous methanol layer (100 L_m). (D) shows the desorption of the same amount of OCS adsorbed on 100 L_m of crystalline methanol.

140 K can be assigned to OCS desorbing as the water undergoes a liquid-phase transition at ∼136 K (Smith & Kay 1999; Souda 2008).

Fig. 2 shows the TPD spectra of OCS desorbing from various configurations of binary OCS/methanol ices. Comparison with Fig. 1 initially suggests that OCS desorption is very different in methanol-dominated ices. In all three cases, there is no evidence of OCS codesorption with methanol ice, which was clearly observed for the water ice (Fig. 1). However, on closer inspection, the two systems exhibit several similarities. OCS desorption from crystalline methanol ice shows a single feature desorbing at approximately 90 K. As for desorption from CI and HOPG, this corresponds to OCS desorption directly from the surface of the methanol ice. The desorption of OCS from the surface of amorphous methanol and from a mixture are very similar, exhibiting two features: a smaller peak at approximately ∼90 K and a sharper peak at ∼112 K. The low-temperature feature can be assigned to OCS desorption from the surface region of the methanol ice, by comparison with desorption from crystalline methanol. The peak at approximately 112 K cannot be assigned by TPD alone and therefore RAIRS was employed to determine the origin of this feature.

Fig. 3 shows RAIR spectra for OCS:methanol ices annealed to various temperatures. The spectra show the OH vibrational band (3300 cm^{-1}) and the CO stretching mode (1040 cm^{-1}) of methanol. A clear change is observed in these regions upon heating the ice to 115 K, including sharpening and splitting of the bands. These observations are indicative of the onset of methanol crystallization (Bolina et al. 2005b). This temperature (115 K) coincides with the desorption of the higher temperature OCS peaks observed in the TPD spectra of layered amorphous and codeposited OCS/methanol binary ices (Fig. 2). The TPD peak observed at 112 K in Fig. 2 can

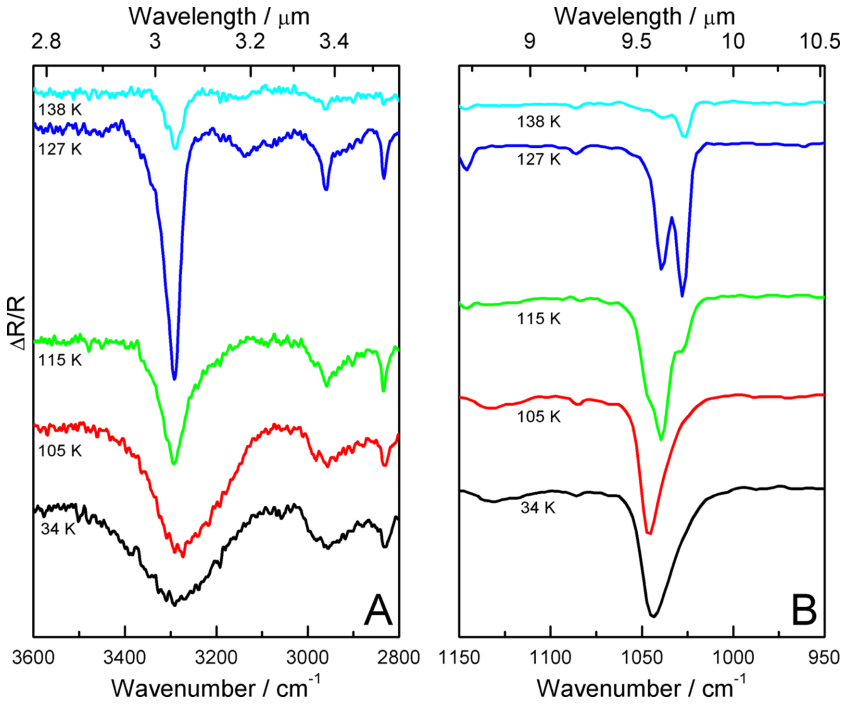

Figure 3. RAIR spectra showing the annealing of 100 L_m of a mixed OCS:methanol ice adsorbed on HOPG. (A) shows the spectral region between 3600 and 2800 cm^{-1} showing the O–H stretch of methanol and (B) shows the region between 1150 and 950 cm^{-1} that highlights the C–O band. The annealing temperatures are shown in the figure.

therefore be attributed to the desorption of OCS from the methanol ice as it undergoes a phase transition (Souda 2004), analogous to the trapping and release observed for OCS binary water ices.

With the behaviour of both water and methanol-dominated binary ices established, Fig. 4 shows TPD spectra recorded for the desorption of water, methanol and OCS from a ∼10:1:1 tertiary ice. Clearly, the desorption behaviour of all three ice components is considerably altered compared to the binary ices. First, the characteristic low-temperature shoulder on the leading edge of the water TPD, indicating the ASW–CI phase transition, is absent. This suggests a change in the crystallization behaviour of ASW. Secondly, both methanol and OCS exhibit complex desorption profiles compared to those observed in the binary ices (Figs 1 and 2). OCS desorption is now dominated by codesorption with water and methanol, rather than volcano desorption. This clearly shows that combining water and methanol changes the trapping mechanism of OCS within the tertiary ice. Furthermore, desorption of OCS and methanol at lower temperatures, extending from 100 K to the codesorption feature at 161 K, is more complex than for the binary ices.

To aid the understanding of these marked changes in the desorption behaviour, infrared spectra were also recorded for the tertiary ices. Fig. 5 shows a comparison of RAIR spectra of the OH stretching region for the tertiary ice (A) and pure water ice (B). This region of the spectrum acts as a fingerprint for the phase transition of water, with distinct spectral changes occurring in the band profile, depending on the extent of crystallization of ASW (Hagen et al. 1981; Backus et al. 2004; Bolina et al. 2005a). As shown in Fig. 5B, pure ASW converts to CI following annealing to 145 K, as indicated by a sharpening and change in the profile of the OH band, accompanied by a shift to lower wavenumber. In contrast, the OH band for the tertiary ices (Fig. 5A) already shows the spectral changes characteristic of the onset of water crystallization following annealing to 125 K. This marked decrease in water crystallization temperature is ascribed to the presence of methanol in the water ice, as previously reported by Souda, who also observed a decrease in crystallization temperature of a water layer when methanol was deposited on top (Souda 2007). This is consistent with the absence of the characteristic shoulder on the leading edge of the water TPD (Fig. 4), which signifies the phase transition. This is also consistent with the lack of OCS and methanol desorption at the water-phase transition temperature of 158 K, which is observed for the binary ices (Figs 1 and 2). Since the water-phase transition for the tertiary ice now takes place at a much lower temperature, it occurs before the water desorbs. Hence, only the desorption of crystalline water is observed during the TPD and therefore only codesorption features are observed for the OCS and methanol in the tertiary ice.

The complex peak, occurring before the main desorption of OCS, is clearly much larger for the tertiary ices than for the binary ices (Fig. 4). The observed complex desorption in both cases most likely arises due to a combination of effects. The low-temperature feature around 100 K can be attributed to OCS diffusion through the methanol:water lattice. This assignment is based on a comparison of OCS desorption from binary layered water ices (Fig. 1) and ices where OCS is deposited on top of a water:methanol mixed ice (discussed later) which show the same desorption feature. In these cases, OCS desorption occurs around its natural sublimation temperature (∼85 K). However, similar desorption is not observed for the OCS:water binary ice mixtures. This suggests that the tertiary ice mixture is more porous than the binary ice, allowing OCS to diffuse through the matrix more readily.

The two additional complex features (Fig. 4C inset) are more difficult to definitively assign with infrared and TPD alone. The higher temperature feature is possibly due to the release of trapped OCS at the modified ASW–CI phase transition which now occurs at lower temperatures (Fig. 5). This is consistent with the observation of a similar feature for CO_2 (Edridge et al. 2013) as discussed later,

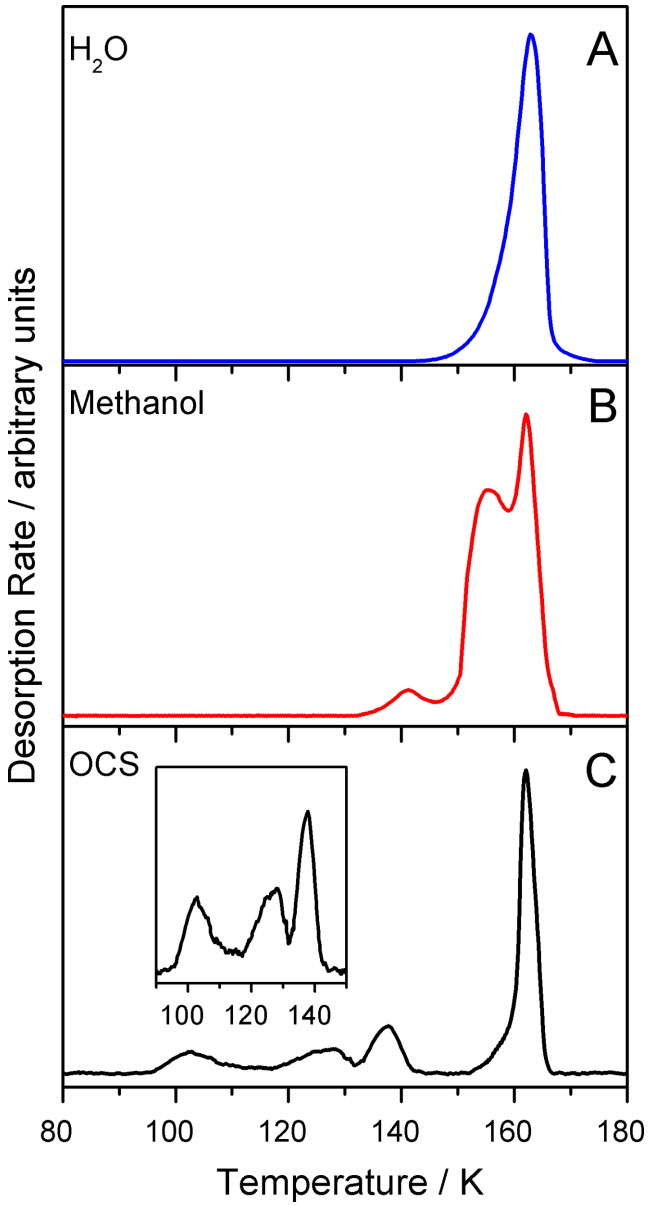

Figure 4. TPD spectra for the desorption of water (A), methanol (B) and OCS (C) from 100 L_m of a tertiary ice with a ratio of 10:1:1 for water, methanol and OCS, respectively. The inset in panel (C) shows an expanded view of the desorption of OCS from 90 to 150 K.

and a coincident peak in the methanol TPD (Fig. 4). In contrast, the peak at ∼125 K is more difficult to definitively assign. However, based on comparison with the binary mixtures, this peak possibly arises from OCS desorption from the ice as ASW undergoes a structural rearrangement at a methanol-modified glass transition temperature.

Methanol desorption from the tertiary ices is also complex in nature. It is characterized by two main peaks at 158 and 152 K and a smaller peak at 140 K. The peak at 158 K coincides with water and OCS desorption and can therefore be assigned to codesorption of the methanol and OCS with water. The 140 K peak is assigned to desorption of methanol at the modified ASW–CI phase transition, and coincides with concurrent OCS desorption, as described above. The methanol peak observed at 152 K is more difficult to definitively assign; however, this has been tentatively assigned to the desorption of pure methanol from the subsurface region of the mixed ice (Burke & Brown 2010).

Clearly, the presence of methanol in the tertiary ice significantly changes the desorption characteristics of OCS. The retention of OCS in the tertiary ices is surprising, since the lowering of the onset of ASW crystallization might be expected to give rise to OCS desorption at lower temperatures corresponding to the modified phase change of ASW (125–135 K). This is clearly not the case, since OCS desorption from the tertiary ices is dominated by codesorption. Therefore, a mechanism must exist whereby OCS is trapped in the ice to higher temperatures. One possibility for this observed trapping is the formation of methanol clathrate hydrate structures, which are known to have the ability to encapsulate other guest molecules within the cage structure (Blake et al. 1991; Ehrenfreund et al. 1999; Notesco & Bar-Nun 2000). The trapped molecules are then released upon clathrate decomposition which occurs on a time-scale of bulk ice desorption, with excess methanol ejected into the gas phase at lower temperatures.

4 DISCUSSION

These observations have clear implications for the modelling of desorption in interstellar regions, such as hot cores (Viti et al. 2004) since these rely on the classification of volatiles according to their desorption characteristics, which in turn are governed by water-phase transitions (Collings et al. 2004). As these data show, methanol changes the phase transition temperature of water ice (Fig. 5) and therefore significantly alters the desorption characteristics of volatile species trapped within these ices. This behaviour is not unique to OCS. Fig. 6 shows TPD spectra following the deposition of 20 L_m of CO_2 ice on top of a 15 per cent methanol:water mixed ice. A 20 L_m OCS TPD spectrum from an identical experiment has been added for comparison. Clearly, Fig. 6 shows that the trapping and desorption behaviour of the two volatile species is almost identical. Both traces show four main features which correspond directly to the features observed for the tertiary OCS:methanol:water ices. Desorption from the surface of the methanol:water ice occurs at low temperature for both species. This peak is considerably larger for the layered ices shown in Fig. 6 compared to the mixed ices seen in Fig. 1, as expected. The highest temperature peak corresponds to codesorption with water ice, which is also observed in the tertiary ice mixtures (Fig. 4). The two complex desorption features at ∼140 K are assigned to the same species as for the mixed ices, i.e. desorption at the modified ASW–CI phase transition (higher temperature peak) and the modified water glass transition (lower temperature peak). Given the similar behaviour observed for CO_2 and OCS, it would be expected that other volatile ice components should give rise to analogous desorption trends. Similar trends have been observed for adsorption on other methanol:water layered ices, where the additional third component, butane (Souda 2007), also gives rise to three complex desorption features between 100 and 150 K, and a shift of the dominant desorption at the ASW–CI phase transition to codesorption with CI. Furthermore, multicomponent ice experiments, which also contain methanol as a key ice constituent, also demonstrate complex desorption behaviour over the same temperature range (Notesco & Bar-Nun 2000; Martín-Doménech et al. 2014).

The data in Fig. 6 also provide further insights into the relevance of laboratory studies of layered ices of astrophysical relevance. It is known that CO accretes on the surfaces of dust grains to form layered ices. CO is considered to be a precursor in the formation of both CO_2 (Goumans et al. 2008; Ioppolo et al. 2011) and OCS

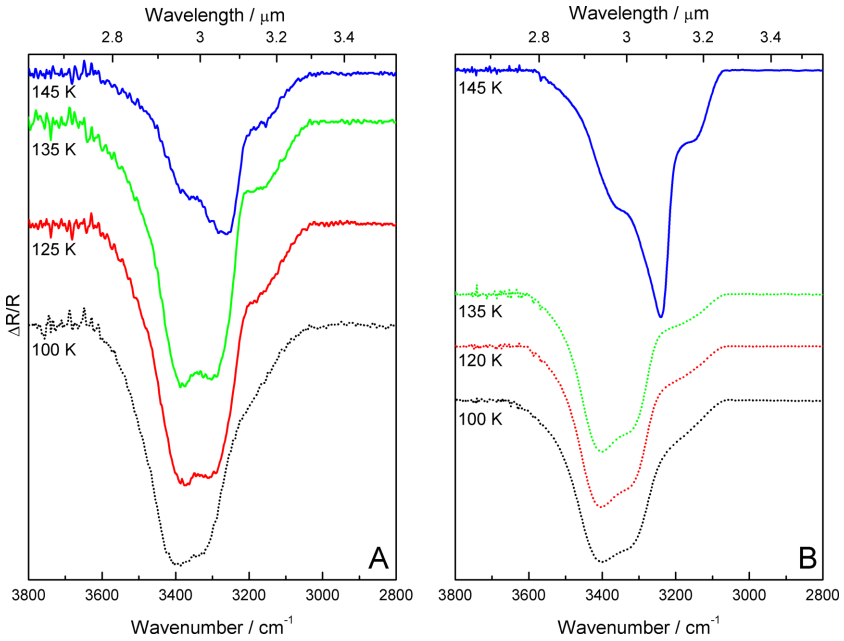

Figure 5. RAIR spectra showing the O–H stretching region for (A) a tertiary ice consisting of OCS, water and methanol and (B) for pure water ice. The dotted lines in each panel indicate the amorphous phase of water ice. The annealing temperatures are shown in the figure.

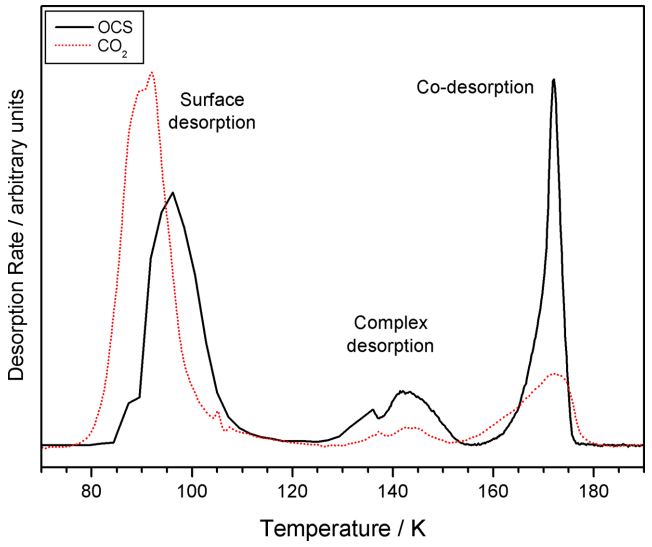

Figure 6. TPD spectra showing the desorption of a 20 L_m exposure of CO_2 (dotted line) deposited on top of a 15 per cent methanol:water ice mixed ice. A 20 L_m OCS TPD trace from an identical experiment has been overlaid for comparison.

(Adriaens et al. 2010; Garozzo et al. 2010) and hence studying layered ices is relevant for both of these species. Experiments show that the layered ice systems exhibit similar behaviour to that of the mixed ices, with all four desorption features being observed in TPD for both ice configurations. Hence, the thermal desorption mechanism of the ices appears to be similar.

The similarity of the mixed and layered tertiary ice systems is further illustrated in Fig. 7, which compares the thermal behaviour of the infrared OCS band in both ices. Fig. 7A shows RAIR spectra for the mixed tertiary OCS:methanol:water ice following sequential annealing. The OCS band is observed at 2048 cm^{-1} irrespective of annealing temperature, with desorption being seen following annealing to 155 K, in agreement with Fig. 4. Fig. 7B shows the same band; however, in this case the OCS ice is deposited on top of a methanol:water mixed ice. At first glance, the spectrum is different compared to Fig. 7A, with a broad infrared band located at 2075 cm^{-1}. This band corresponds to the infrared stretch of pure OCS ice (Burke & Brown 2010). However, closer inspection shows that once the surface-bound OCS species has desorbed at 95 K, the OCS band shifts to 2048 cm^{-1} resulting in a spectrum in agreement with that observed for the mixed tertiary ice. This result confirms that the underlying thermal processing and trapping of the layered and mixed systems are equivalent once the surface-bound species has desorbed.

5 ASTROPHYSICAL IMPLICATIONS

To place the experimental data in an astrophysical context, we employ a simple model to simulate the desorption of OCS ices on astrophysical time-scales and at interstellar dust temperatures. The purpose of the model is not to provide a direct extrapolation of laboratory data to astrophysical processes, which requires a more rigorous and detailed approach to incorporate a wide scope of complexities, but rather to give a rough estimate of desorption temperatures and time-scales of the modified OCS desorption profile from binary and tertiary ices. This simple model has been used previously to describe the desorption of the three structural isomers of $C_2O_2H_4$ as pure ices and from mixed water-rich ices containing 1 per cent of the isomer (Burke et al. 2015). Briefly, the model incorporates experimental observations of the desorption behaviour (the sublimation phases) of the ices in addition to experimentally derived kinetic parameters for the desorption. These are combined with astrophysically relevant, non-linear, heating rates and ice thicknesses to model thermal desorption under interstellar conditions.

As previously, the ice thickness used in the model is based on estimates of ices that accrete on interstellar grains as used previously (Brown & Bolina 2007). The total ice thickness is set to 0.3 μm, corresponding to an initial surface coverage of 9.5×10^{21} mol m^{-2}. The

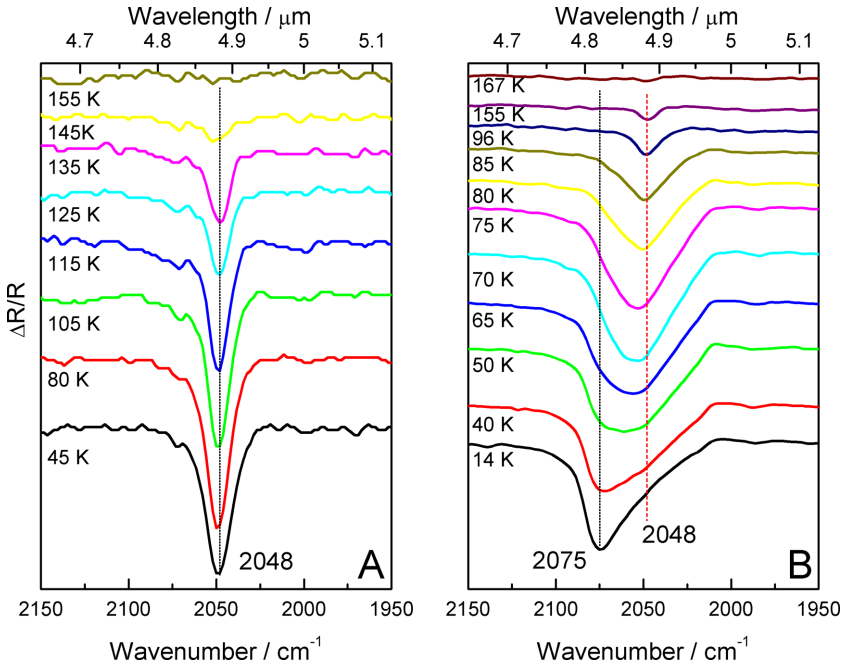

Figure 7. RAIR spectra showing the CO vibration following the sequential annealing of OCS adsorbed in (A) a tertiary mixed ice consisting of OCS:methanol:water and (B) a layered ice consisting of OCS on top of a methanol:water ice. The annealing temperatures are shown in the figure.

Table 1. Kinetic parameters used to simulate OCS desorption from binary water-rich ices and tertiary OCS:water:methanol ices. Data for OCS were derived from our own experimental data (Burke & Brown 2010). Parameters for ASW and CI are those determined previously (Fraser et al. 2001). The modified volcano desorption parameters were derived by calculating a scaled desorption energy from the ASW kinetic parameters. Note that the units for the pre-exponential factor are for zero-order desorption.

Molecule	Desorption energy, E_{des}		Desorption order, n	Pre-exponential factor, ν/mol m^{-2} s^{-1}
	(K)	(kJ mol^{-1})		
OCS	3440	28.6	0.11	4.2×10^{32}
ASW	5605	46.6	0.01	1.0×10^{34}
CI	5761	47.9	0.01	1.0×10^{34}
Modified volcano	4667	38.8	0.01	1.0×10^{34}

exact composition of the ice configurations modelled is discussed below. Laboratory linear heating rates of 0.5 K s^{-1} are replaced by non-linear heating rates that are dependent on both the temperature and mass of the nearby star which heats the grain. In our model, we apply heating rates for 5, 25 and 60 $M_\odot$ as derived previously (Viti et al. 2004).

The rate of desorption of the ice is described by the Polanyi–Wigner equation (de Jong & Niemantsverdriet 1990). This is trivial when modelling pure OCS ice desorption, which uses kinetic parameters obtained from leading edge analysis of pure ices (Burke & Brown 2010). However, it is clear from Figs 1, 4 and 6 that both the binary and tertiary ices give rise to additional OCS desorption components as a result of trapping and release in the respective ices. Since these desorption events are controlled by the water and water:methanol ices, the kinetic parameters for pure OCS cannot be applied to describe this desorption process. Hence, OCS desorption in the binary and tertiary ices that is assigned to volcano and codesorption is modelled using kinetic parameters for ASW and CI, respectively. The kinetic parameters used in both cases are detailed in Table 1 and were derived previously (Fraser et al. 2001). The remaining OCS desorption features observed in the tertiary layered and mixed ices assigned to desorption via a modified volcano mechanism and a modified water glass transition are more difficult to model accurately. However, since desorption in both cases is dictated by modified phase transitions of water, for simplicity we have combined the two processes and derived a set of desorption kinetics for a single component using the parameters for ASW desorption as a basis. In this case, the desorption energy, E_{des}, was scaled in order to generate a desorption temperature that matched our experimental observations. The resulting kinetics from these calculations are also detailed in Table 1.

To simulate desorption of the mixed ices, the percentage of each desorption component was determined from the experimental data by integrating the areas under the TPD peaks. The percentages obtained are shown in Table 2. The percentages were derived from repeated experiments where the ice composition was approximately 10–15 per cent with respect to OCS. For the layered systems, corresponding 10–15 L_m exposures of OCS adsorbed on water or on water:methanol were used to calculate the percentages of each desorption component.

The composition of the model ices was dependent on the ice configuration. For the binary ices, the composition was 99 per cent

Table 2. Calculated percentages for each desorption phase from the binary and tertiary layered and mixed ice configurations. The percentages are derived from integrating the areas under the TPD curves and are obtained from repeated experiments.

Desorption phase	Ice configuration			
	Binary		Tertiary	
	Layered	Mixed	Layered	Mixed
Surface	28%	6%	48%	9%
Modified volcano	–	–	17%	26%
Volcano	71%	89%	–	–
Codesorption	1%	5%	34%	65%

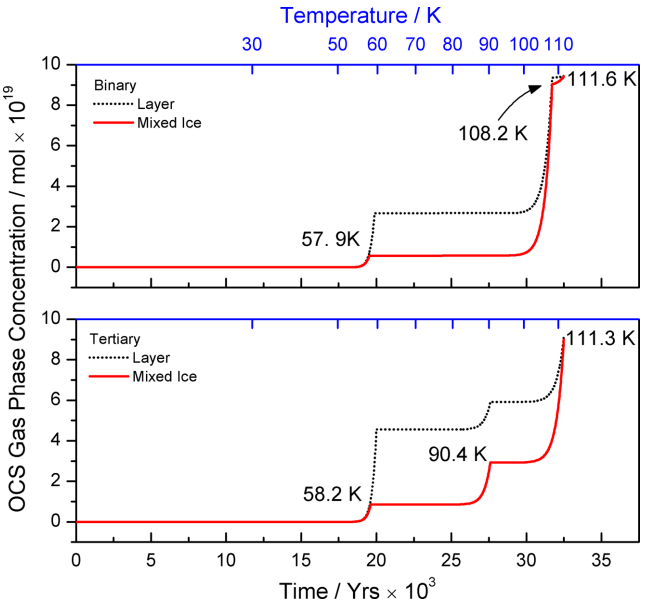

Figure 8. Concentration profiles showing the evolution of OCS into the gas phase from layered and mixed ices for a 25 $M_\odot$ star as a function of time (bottom axis) and temperature (top axis). The top panel shows the results of simulated desorption for binary OCS:water ices comprising 1 per cent OCS. The bottom panel shows the results for a tertiary OCS:methanol:water ices comprising 1 per cent OCS, 15 per cent methanol and 84 per cent water. The temperatures marked on the figure correspond to the desorption processes for the mixed ices in each case.

with respect to water, with the remaining 1 per cent of the molecules corresponding to OCS. For the tertiary ices, the composition was altered to account for the inclusion of methanol, giving 84, 15 and 1 per cent for water, methanol and OCS, respectively. The 1 per cent of the ice corresponding to the OCS in the mixed ices is then ratioed according to the percentages listed in Table 2, and the respective desorption kinetics derived in Table 1 are applied to model each desorption phase.

Fig. 8 shows the results of the simulation for the binary OCS:water and tertiary OCS:water:methanol ices for both layered and mixed ice configurations. For clarity, only data for 25 $M_\odot$ are shown. The simulated desorption temperatures and times for all three star masses are detailed in Table 3. It is immediately clear that the desorption temperatures on astrophysical time-scales are lower compared to the laboratory desorption temperatures, even when considering the thicker ices used in the simulation (which would yield higher temperatures in the laboratory). When considering a 25 $M_\odot$ star, the temperatures of surface, modified volcano, volcano and codesorption are 58, 90, 108 and 111 K. These compared to the respective experimental values of 102, 138 and 162 K for the surface, modified volcano and codesorption peaks observed for a tertiary ice. As clearly seen in Fig. 8, the effect of the addition of methanol to the ice (either as a layer or in a mixture) is to cause larger amounts of OCS to be released from the ice mantle at lower temperatures and earlier times. This earlier release occurs as a result of the lowering of the temperature of the methanol-modified water-phase transition. The behaviour across all three star masses considered here is similar, although clearly desorption occurs much more rapidly for 60 $M_\odot$ compared to 25 and 5 $M_\odot$, as seen in Table 3. However, due to the different heating rates of the three star masses studied, the temperatures of the different phases of OCS desorption are also modified for the different star masses. Whilst this is a very simple model that needs to be confirmed by more detailed astrophysical models, it is clear that this earlier release of OCS will have profound implications for detected OCS gas-phase concentrations.

6 CONCLUSIONS

Binary ices dominated by water do not provide a complete picture of thermal desorption. More complex ices, although experimentally challenging, must also be considered to successfully model astrophysical ices and the evolution of gas-phase species in chemically rich star-forming regions. Methanol is shown to not only change the crystallization kinetics of ASW, by lowering the temperature of the phase change, but also gives rise to marked changes in the trapping and release of guest molecules. Significantly, release of volatiles traditionally observed in binary water-dominated ices occurs at the ASW–CI phase transition, whereas tertiary ices containing water and methanol change this process to predominantly codesorption with the bulk ice. Whilst the exact mechanisms of these observed changes require further study, it is clear that astrophysical models of the desorption of interstellar and cometary ices must consider the

Table 3. Simulated desorption temperatures (T) with corresponding times (t) for the different phases of OCS desorption from binary and tertiary mixed ices as a function of star mass. The composition of the binary and tertiary ice is 1 per cent with respect to OCS.

Star mass/$M_\odot$		Binary mixture			Tertiary mixture		
		Surface	Volcano	Codesorption	Surface	Modified volcano	Codesorption
60	T (K)	58.7	110.4	113.9	59.1	92.2	113.6
	$t\,10^5$ (yr)	0.122	0.168	0.171	0.123	0.154	0.171
25	T (K)	57.9	108.2	111.6	58.2	90.4	111.3
	$t\,10^5$ (yr)	0.195	0.317	0.325	0.196	0.276	0.325
5	T (K)	55.9	103.1	106.3	56.2	86.4	106.0
	$t\,10^5$ (yr)	0.783	2.08	2.19	0.790	1.57	2.19

changed trapping and desorption behaviour of small volatiles that is caused by the presence of methanol in the ice.

ACKNOWLEDGEMENTS

This work was performed at University College London (UK) and the Leverhulme Trust is thanked for funding for DJB. Stefano Belbin is thanked for his assistance in performing preliminary OCS adsorption and desorption experiments. Serena Viti is thanked for critical reading of the manuscript.

REFERENCES

Adriaens D. A., Goumans T. P. M., Catlow C. R. A., Brown W. A., 2010, J. Phys. Chem. C, 114, 1892
Ayotte P., Smith R. S., Stevenson K. P., Dohnálek Z., Kimmel G. A., Kay B. D., 2001, J. Geophys. Res., 106, 387
Backus E., Grecea M., Kleyn A., Bonn M., 2004, Phys. Rev. Lett., 92, 236101
Bar-Nun A., Kleinfeld I., Kochavi E., 1988, Phys. Rev. B, 38, 7749
Blake D., Allamandola L., Sandford S., Hudgins D., Freund F., 1991, Science, 254, 548
Bockelee-Morvan D et al. 2000, A&A, 1114, 1101
Bolina A. S., Wolff A. J., Brown W. A., 2005a, J. Phys. Chem. B, 109, 16836
Bolina A. S., Wolff A. J., Brown W. A., 2005b, J. Chem. Phys., 122, 44713
Boogert A. C. A., Tielens A. G. G. M., Ceccarelli C., Boonman A. M. S., van Dishoeck E. F., Keane J. V., 2000, A&A, 360, 683
Brown W. A., Bolina A. S., 2007, MNRAS, 374, 1006
Burke D. J., Puletti F., Brown W. A., Woods P. M., Viti S., Slater B., 2015, MNRAS, 447, 1444
Burke D. J., Brown W. A., 2010, Phys. Chem. Chem. Phys., 12, 5947
Codella C., Viti S., Williams D. A., Bachiller R., 2006, ApJ, 644, L41
Collings M. P., Anderson M. A., Chen R., Dever J. W., Viti S., Williams D. A., McCoustra M. R. S., 2004, MNRAS, 354, 1133
Cruikshank D. P et al. 1998, Icarus, 135, 389
Dartois E., Schutte W., Geballe T. R., Demyk K., Ehrenfreund P., d'Hendecourt L., 1999, A&A, 35342, L32
De Jong A. M., Niemantsverdriet J. W., 1990, Surf. Sci., 233, 355
DelloRusso N., Disanti M. A., Mumma M. J., Magee-Sauer K., Rettig T. W., 1998, Icarus, 135, 377
Edridge J. L., Freimann K., Burke D. J., Brown W. A., 2013, Phil. Trans. R. Soc. A, 371, 20110578
Ehrenfreund P., d'Hendecourt L., Dartois E., Jourdain de Muizon M., Breitfellner M., Puget J. L., Habing H. J., 1997, Icarus, 130, 1
Ehrenfreund P et al. 1999, A&A, 253, 240
Fraser H. J., Collings M. P., McCoustra M. R. S., Williams D. A., 2001, MNRAS, 327, 1165
Garozzo M., Fulvio D., Kanuchova Z., Palumbo M. E., Strazzulla G., 2010, A&A, 67, 509
Gibb E. L et al. 2000, ApJ, 536, 347
Goumans T. P. M., Uppal M. A., Brown W. A., 2008, MNRAS, 384, 1158
Grim R. J. A., Bass F., Geballe T. R., Greenberg J. M., Schutte W., 1991, A&A, 243, 473
Hagen W., Tielens A. G. G. M., Greenberg J. M., 1981, Chem. Phys., 56, 367
Herbst E., van Dishoeck E. F., 2009, ARA&A, 47, 427
Ioppolo S., van Boheemen Y., Cuppen H. M., van Dishoeck E. F., Linnartz H., 2011. MNRAS, 413, 2281
Jewitt D. C., Luu J., 2004, Nature, 432, 731
Klinger J., 1983, J. Phys. Chem., 87, 4209
Lellouch E et al. 1995, Nature, 373, 592
Martín-Doménech R., Muñoz Caro G. M., Bueno J., Goesmann F., 2014, A&A, 564, A8
Merlin F., Guilbert A., Dumas C., Barucci M. A., de Bergh C., Vernazza P., 2007, A&A, 466, 1185
Merlin F., Quirico E., Barucci M. A., de Bergh C., 2012, A&A, 540, 1
Mills F., Esposito L., Yung Y., 2007. in Esposito L., Stofan E., Cravens T. (eds), Exploring Venus As A Terrestrial Planet. American Geophysical Union, Washington, DC, p. 176
Notesco G., Bar-Nun A., 2000, Icarus, 148, 456
Palumbo M. E., Geballe T. R., Tielens A. G. G. M., 1997, 20, 839
Palumbo M. E., Tielens A. G. G. M., Tokunaga A. T., 1995, ApJ, 449, 674
Pontoppidan K. M., Dartois E., van Dishoeck E. F., Thi W.-F., D'Hendecourt L., 2003, A&A, 20404, L17
Smith R. S., Kay B. D., 1999, Nature, 398, 788
Smith R. S., Huang C., Wong E. K. L., Kay B. D., 1997, Phys. Rev. Lett., 79, 909
Souda R., 2004, Phys. Rev. Lett., 93, 235502
Souda R., 2007, Phys. Rev. B, 75, 184116
Souda R., 2008, J. Chem. Phys., 129, 124707
Viti S., Collings M. P., Dever J. W., McCoustra M. R. S., Williams D. A., 2004, MNRAS, 354, 1141
Whittet D. C. B., 1993, in Millar T. J., Williams D. A. (eds), Dust and Chemistry in Astronomy. IoP Publishing, Bristol, p. 9
Wolff A. J., Carlstedt C., Brown W. A., 2007, J. Phys. Chem. C, 111, 5990
Yung Y. L., Liang M. C., Jiang X., Shia R. L., Lee C., Bézard B., Marcq E., 2009, J. Geophys. Res., 114, E00B34

This paper has been typeset from a TEX/LATEX file prepared by the author.